Saturation *versus* inductive effects: the electrochemistry of the $C_{70}Ph_{2n}$ (n = 1–5) series

Anthony G. Avent,[a] Paul R. Birkett,*[a] Maurizio Carano,[b] Adam D. Darwish,[a] Harry W. Kroto,[a] Jaime Oviedo Lopez,[b] Francesco Paolucci,*[b] Sergio Roffia,[b] Roger Taylor,[a] Norbert Wachter,[a] David R. M. Walton[a] and Francesco Zerbetto*[b]

[a] *School of Chemistry, Physics & Environmental Sciences, Sussex University, Brighton, UK BN1 9QJ*

[b] *Dipartimento di Chimica "G. Ciamician", Università degli Studi di Bologna, via F. Selmi 2, 40126 Bologna, Italy*

Received (in Cambridge, UK) 26th January 2000, Accepted 4th December 2000
First published as an Advance Article on the web 8th January 2001

Several arylfullerenes, $C_{70}Ph_{2n}$ (n = 1–5), are characterised. Their electrochemical properties, investigated by cyclic voltammetry, are the result of a competition between the electron-withdrawing effect exerted by the phenyl groups and the destabilization of redox orbitals deriving from the saturation of double bonds. $C_{70}Ph_2$ is easier to reduce than C_{70}, a feature possibly shared with $C_{70}Ph_4$ that makes these derivatives of C_{70} amongst the best electron acceptor molecules so far discovered. In the following derivatives, destabilization prevails, and reductions become increasingly more cathodic along the series. NMR spectroscopy is used to investigate $C_{70}Ph_{2n}$ (n = 1–3). Finally, calculation of the LUMO energies supports the earlier reduction of $C_{70}Ph_2$ and calculations also indicate the layering of the injected charges, in the multiply-reduced species, over concentric shells.

Introduction

Carbon-based systems carry distinctive electronic properties that make them fundamental building blocks for materials science. The archetypal family spans include ethylene to polyenic linear chain, benzene to aromatic tiles, and spheroids of various sizes (fullerenes). The combination and the interaction between these prototypical moieties can be used to select or tune properties of interest. [70]Fullerene (C_{70}), the second most common fullerene, can form a series of phenylated derivatives of the type $C_{70}Ph_{2n}$, with n = 1–5. Insertion of a phenyl group into C_{70} saturates a carbon atom in the cage and can modify its electronic properties. A number of effects can differentiate $C_{70}Ph_{2n}$ from C_{70}: (i) (extensive) saturation of the cage atoms decreases π-electron conjugation and can effectively render its electronic properties closer to those of planar systems; (ii) the phenyl groups can pull electrons from the central fullerene unit through inductive ($-I$) effects and make them even better electron acceptors; (iii) (quasi-)degeneracy of the cage and phenyls' π-electron systems can spread over the entire molecule, the delocalisation affecting the nature of the electronic states; (iv) subtle (push-pull) effects[1] can become operative and modify the higher order molecular responses (β and γ are the properties most likely to be enhanced); (v) the solid-state external dynamics of fullerenes, in which the pristine spheroids spin at room temperature 10^9–10^{10} times per second,[2] are substituted by the internal dynamics of the phenyl rotors, which are carried over to the isolated phase and solution and may affect other properties, such as lifetimes of electronically excited states.

The interplay between the C_{70} cage and an increasing number of phenyl groups can therefore provide novel interesting properties, the variation of which along the series may not be smooth. In an effort to characterise the electronic properties of these materials, a combined electrochemical and computational investigation was carried out to elucidate the competition between the electron withdrawal by the phenyl groups and the saturations they bring to the cage.

Experimental

Materials

$C_{70}Ph_2$, $C_{70}Ph_4$ and $C_{70}Ph_6$ were obtained as minor by-products during the synthesis of $C_{70}Ph_8$ from $C_{70}Cl_{10}$ using the published procedures.[3] The crude reaction mixture was subjected to column chromatography. Elution with cyclohexane gave a mixture of C_{70} and $C_{70}Ph_2$, $C_{70}Ph_4$ (green solution, R_f = 0.47) and $C_{70}Ph_6$ (yellow brown solution, R_f = 0.21). $C_{70}Ph_8$ and $C_{70}Ph_{10}$ were eluted subsequently using 1:1 cyclohexane–toluene. The mixture of C_{70} and $C_{70}Ph_2$ was rechromatographed (SiO_2, cyclohexane) on a longer column, resulting in the elution of C_{70}, followed by $C_{70}Ph_2$ as a wine-red fraction (R_f = 0.76).

7,19-Diphenyl-7,19-dihydro[70]fullerene. ν_{max}(KBr)/cm^{-1} 3056, 3026, 1597, 1552, 1531, 1490, 1478, 1461, 1445, 1432, 1404, 1385, 1347, 1272, 1228, 1185, 1155, 1078, 1031, 1002, 908, 901, 865, 836, 792, 778, 760, 742, 732, 727, 717, 712, 693, 676, 664, 640, 588, 584, 574, 567, 553, 530, 525, 494, 487, 477, 469, 443; ^{1}H NMR [500 MHz; $CDCl_3$ (lock)] δ_H 7.084–7.123 (4 H, dd, *meta*-H), 7.142–7.176 (2 H, tt, *para*-H), 7.287–7.321 (4 H, dd, *ortho*-H); EI-MS *m*/*z* 994 (M^+ for $C_{70}Ph_2$, 19%), 917 ($C_{70}Ph$, 16%) and 840 (C_{70}, 100%).

7,19,23,37-Tetraphenyl-7,19,23,37-tetrahydro[70]fullerene. ν_{max}(KBr)/cm^{-1} 3056, 3025, 1598, 1572, 1537, 1492, 1470, 1462, 1445, 1438, 1413, 1384, 1353, 1301, 1271, 1256, 1228, 1205, 1186, 1156, 1079, 1044, 1031, 1003, 949, 931, 875, 838, 802, 787, 757, 747, 742, 733, 724, 713, 693, 683, 678, 662, 654, 643, 618, 593, 585, 577, 569, 551, 538, 526, 517, 513, 471; ^{1}H NMR [500 MHz; CD_2Cl_2 (lock)] δ_H 6.938–6.969 (4 H, dd, *meta*-B), 7.042–7.077 (2 H, tt, *para*-B), 7.162–7.223 (6 H, m, *ortho*- and *para*-A), 7.257–7.283 (4 H, dd, *ortho*-B) and 7.565–7.586 (4 H, m, *ortho*-A); ^{13}C NMR [125.76 MHz; CS_2/$CDCl_3$ (lock)] δ_C (number of carbon atoms) 60.05 (2C), 60.56 (2C), 127.17 (2C), 127.63 (2C), 127.72 (4C), 128.06 (4C), 128.26 (4C), 128.41 (2C), 128.85 (4C), 130.23, 130.37 (2C), 130.56 (2C), 135.43 (2C), 136.07 (2C),

 DOI: 10.1039/b000754o

137.441 (2C, *ipso*), 138.84 (2C, *ipso*), 138.98 (2C), 140.51 (2C), 142.62 (2C), 142.65 (2C), 143.32 (2C), 143.35 (2C), 143.50 (2C), 143.76 (2C), 144.38 (2C), 144.91 (2C), 144.98 (2C), 145.03 (2C), 145.70 (2C), 146.16 (2C), 146.93 (2C), 147.16 (2C), 147.35 (1C), 147.67 (2 × 2C), 148.15 (1C), 149.08 (2C), 149.51 (2C), 149.71 (2 × 2C), 149.77 (1C), 149.88 (2C), 150.05 (2C), 150.93 (1C), 152.62 (2C), 152.92 (2C), 163.22 (2C); EI-MS *m*/*z* 1149 (M^+ for $C_{70}Ph_4$, 28%), 1072 ($C_{70}Ph_3$, 20%), 994 ($C_{70}Ph_2$, 2%) 917 ($C_{70}Ph$, 17%) and 840 (C_{70}, 100%).

7,19,23,37,44,53-Hexaphenyl-7,19,23,37,44,53-hexahydro-[70]fullerene. ν_{max}(KBr)/cm^{-1} 3082, 3056, 3023, 1597, 1583, 1533, 1492, 1446, 1384, 1335, 1272, 1225, 1185, 1156, 1079, 1051, 1032, 1003, 963, 951, 922, 908, 856, 840, 808, 788, 776, 749, 742, 733, 714, 694, 683, 663, 653, 619, 596, 591, 583, 575, 565, 549, 545, 531, 523, 515, 502, 472, 445; ^{1}H NMR [500 MHz; CS_2/$(CD_3)_2CO$ (lock)] δ_H 6.853–6.892 (4 H, dd, *meta*-C), 6.989–7.067 (2 H, tt, *para*-C), 7.018–7.067 (4 H, dd, *meta*-B), 7.095–7.129 (2 H, tt, *para*-B), 7.189–7.215 (4 H, dd, *ortho*-C), 7.215–7.249 (6 H, m, *meta*- and *para*-A), 7.441–7.488 (4 H, dd, *ortho*-B) and 7.638–7.667 (4 H, dd, *ortho*-A); ^{13}C NMR [125.76 MHz; CS_2/$(CD_3)_2CO$ (lock)] δ_C (number of carbon atoms) 60.45 (2C), 60.57 (2C), 61.30 (2C), 127.06 (Ph), 127.16 (Ph), 127.67 (Ph), 127.75 (Ph), 128.08 (Ph), 128.26 (Ph), 128.34 (Ph), 128.85 (Ph), 129.01 (Ph), 131.20 (Ph), 132.00 (2C), 133.62 (2C), 136.19 (2C), 137.23 (2C), 137.55 (2C, *ipso*), 138.08 (2C, *ipso*), 138.36 (2C), 139.03 (2C, *ipso*), 140.26 (2C), 140.77 (2C), 142.94 (2C), 142.96 (2C), 144.12 (2C), 145.06 (2C), 145.87 (2C), 145.94 (2C), 146.21 (2C), 146.31 (2C), 146.67 (2C), 146.72 (2C), 148.25 (2C), 148.47 (2C), 148.98 (1C), 149.06 (2 × 2C), 150.55 (1C), 150.97 (2C), 151.031 (2C), 151.10 (3C), 151.58 (1C), 151.98 (2C), 152.06 (2C), 153.76 (1C), 154.84 (2C), 163.97 (2C); EI-MS *m*/*z* 1303 (M^+ for $C_{70}Ph_6$, 45%), 1226 ($C_{70}Ph_5$, 15%), 1149 ($C_{70}Ph_4$, 1%), 1072 ($C_{70}Ph_3$, $C_{88}H_{15}$, 15%), 994 ($C_{70}Ph_2$, 3%) 917 ($C_{70}Ph$, 33%) and 840 (C_{70}, 100%).

Electrochemistry

TBAH (puriss. from FLUKA) was used as received as the supporting electrolyte. THF (LiChrosolv, Merck) was heated under reflux over sodium, and the solvent was then distilled into a Schlenk vessel containing sodium and benzophenone. After stirring for at least 24 h, a deeply violet solution was obtained, indicating the formation of benzophenone dianion. This mixture was heated under reflux for several hours before the solvent was distilled into a second Schlenk vessel containing sodium and anthracene. Upon stirring, a deeply blue solution was obtained, corresponding to the formation of the anthracene dianion. The solution was then transferred into a third Schlenk vessel, suitably designed for its connection to the electrochemical cell, to remove the excess sodium. This THF solution of sodium anthracenide was stored under reduced atmosphere.[4] All the distillations and transferring procedures were carried out under argon or reduced atmosphere. For the electrochemical experiments the THF was distilled, prior to use, into the electrochemical cell using a trap-to-trap procedure.

Electrochemical instrumentation and measurements. The one-compartment electrochemical cell was of airtight design with high-vacuum glass stopcocks fitted with either Teflon or Kalrez (DuPont) O-rings in order to prevent contamination by grease. The connections to the high-vacuum line and to the Schlenck tube containing the solvent were *via* spherical joints also fitted with Kalrez O-rings. The pressure measured in the electrochemical cell prior to performing the trap-to-trap distillation of the solvent was typically 1.0–2.0 × 10^{-5} mbar.† The working electrode consisted either of a 0.6 mm-diameter platinum wire (*ca*. 0.15 cm^2) sealed in glass or a Pt disc ultramicroelectrode (r = 5 μm) also sealed in glass. The counter-electrode consisted of a platinum spiral and the quasi-reference electrode was a silver spiral. The quasi-reference electrode drift was negligible during the time required by a single experiment. Both the counter and the reference electrodes were separated from the working electrode by ~0.5 cm. Potentials were measured with the ferrocene standard and are always referred to saturated calomel electrode (SCE). $E_{1/2}$ values correspond to $(E_{pc} + E_{pa})/2$ from CV. In some experiments a SCE reference electrode was used, separated from the working electrode compartment by a sintered glass frit. Ferrocene was also used as an internal standard for checking the electrochemical reversibility of a redox couple.

Voltammograms were recorded with a AMEL Model 552 potentiostat or a custom made fast potentiostat controlled by either a AMEL Model 568 function generator or a ELCHEMA Model FG-206F. Data acquisition was performed by a Nicolet Model 3091 digital oscilloscope interfaced to a PC. Temperature control was accomplished within 0.1 °C with a Lauda Klein-Kryomat thermostat. All the experiments were carried out at 25 °C and with a scan rate of 0.5 V s^{-1}.

Computational procedure

The molecular geometries were optimised with the MM3 force field.[5] All the molecular mechanics calculations were run with the Tinker program[6] that has found wide application in our laboratory.[7] Electronic structure calculations were performed at the MNDO level[8] using the *Gaussian 94* suite of programs.[9]

Results and discussion

The structures of $C_{70}Ph_{2n}$ (n = 4 and 5) (Fig. 1) were previously determined by NMR spectroscopy and can be related to lower members of the series (n = 1–3) provided that the addend sites in $C_{70}Cl_{10}$ are maintained in the new derivatives.[3] The new derivatives were initially characterised by EI mass spectrometry, and NMR studies were used to show that each of the $C_{70}Ph_{2n}$ (n = 1–3) compounds possess C_s symmetry. Analysis of the foregoing results infers that the number of possible regio-isomers of $C_{70}Ph_{2n}$ (n = 1–3) decreases as n increases. For these reasons the analysis of $C_{70}Ph_6$ is considered first.

$C_{70}Ph_6$ exhibits three sets of *ortho*-proton NMR signals of equal intensity at δ = 7.189–7.215, 7.441–7.488 and 7.638–7.667, respectively, showing that there are two sets of three freely rotating (in solution) phenyl groups situated about the symmetry plane of the molecule. The C_s symmetry of the molecule is further confirmed by the ^{13}C NMR spectrum which, although it does not exhibit the necessary number of sp^2 signals (probably due to signal co-incidence), has the required three sp^3 carbon signals, each of which has a similar chemical shift; δ = 60.45, 60.57 and 61.30, respectively. The observed free rotation of the six phenyl groups, combined with the similar values for the sp^3 cage carbon signals, rules out the presence of phenyl groups attached to adjacent carbons of the cage. Such a situation in $C_{70}Ph_{10}$, for example, induced a downfield shift in

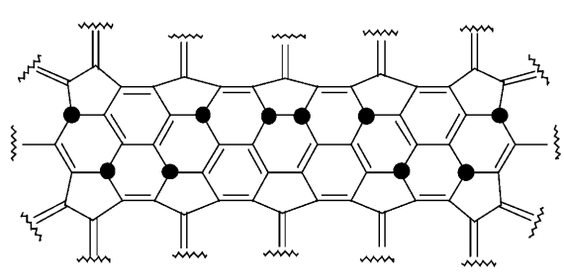

Fig. 1 The waist section of $C_{70}Ph_{10}$ showing the phenyl sites (●). The structure of $C_{70}Ph_8$ is obtained by replacing the two adjacent phenyl groups with a double bond.

† 1 mbar = 100 Pa.

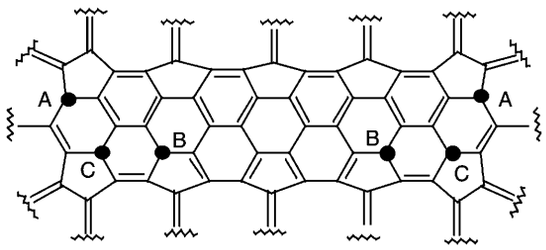

$C_{70}Ph_6$ isomer a, Energy 958.045 kcal mol^{-1}

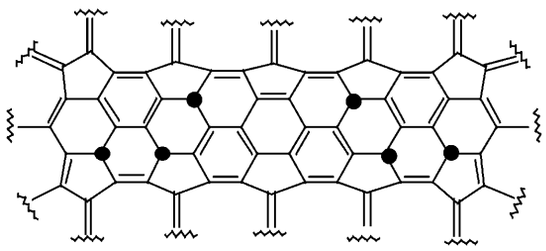

$C_{70}Ph_6$ isomer b, Energy 954.896 kcal mol^{-1}

Fig. 2 The waist section of the two isomers of $C_{70}Ph_6$ showing phenyl sites (●) that satisfy the NMR data. The phenyl rings are labelled A, B and C in the preferred isomer (structure a). The energy values (kcal mol^{-1}) were calculated by optimising the structures using a silicon Graphics Indy 2000 workstation.

one sp^3 carbon signal and, moreover, resulted in the hindered rotation of the pair of adjacent phenyl groups.[3b] Further information regarding the location of the phenyl groups can be obtained from NOE experiments involving the *ortho* protons of each set of phenyl groups. Each of the signals due to the *ortho* protons for the phenyl rings A [$\delta = 7.638$–7.667 (see Fig. 2a for labelling)] and B ($\delta = 7.441$–7.488) have positive NOEs of 2.4 and 1.8%, respectively, with the *ortho*-protons' signal of the phenyl rings C ($\delta = 7.189$–7.215), but not with each other. The *ortho* protons of the phenyl rings C have the reciprocal NOEs with each of the *ortho*-proton signals of the outer pairs of the phenyl rings A and B. The data shows, therefore, that there are three successively 1,4-situated phenyl groups, which span six-membered rings of the cage. The four key facts in assigning a preferred structure for $C_{70}Ph_6$ are therefore that the molecule must; i) have C_s symmetry, ii) use six of the ten addition sites in $C_{70}Cl_{10}$, iii) avoid adjacency of phenyl groups and iv) have two sets of three 1,4-located phenyl groups. There are two possible $C_{70}Ph_6$ regioisomers that satisfy all of these criteria (Fig. 2).[10] The former isomer, 7,19,23,37,44,53-hexaphenyl-7,19,23,37,44,53-hexahydro[70]fullerene, (Fig. 2a) is the most likely, even though it is not the preferred thermodynamic product, as it results from sequential 1,4-substitutions of six chlorine atoms in $C_{70}Cl_{10}$, combined with the necessary elimination of the remaining four chlorines. The latter, by contrast, requires substitution to start at two different chlorine addend sites and, if this were possible, a mixture of both regioisomers would be the expected outcome. Finally, it is worth noting that there are three different combinations of six substitution sites (of the possible ten) capable of generating the former regioisomer.

The C_s symmetry of $C_{70}Ph_4$ is clearly indicated by both the ^{1}H and ^{13}C NMR spectra. Furthermore, the ^{1}H NMR spectrum again shows that the phenyl groups are rotating freely in solution. The ^{13}C NMR spectrum exhibits the required number of signals; two sp^3 signals of similar chemical shift, $\delta = 60.05$ and 60.56, and thirty-one sp^2 signals, each integrating for two carbon atoms. In addition, there are four on-symmetry-plane carbon atoms, each of which appear as half-intensity signals. NOE experiments show that the *ortho* protons of the two sets of phenyl rings are in close proximity. Thus, the structure must

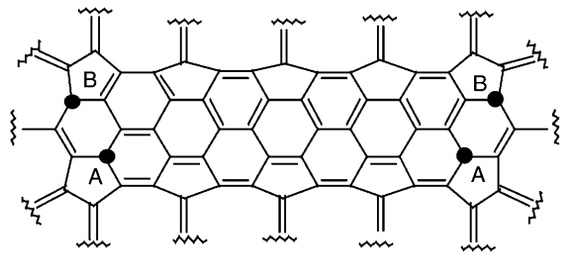

$C_{70}Ph_4$ isomer a, Energy 993.935 kcal mol^{-1}

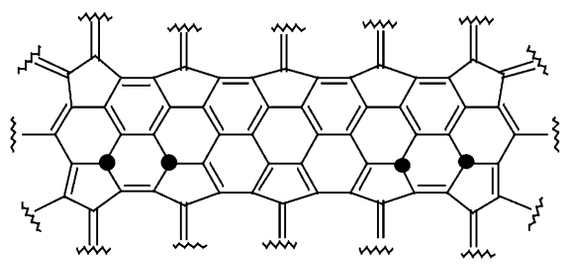

$C_{70}Ph_4$ isomer b, Energy 998.653 kcal mol^{-1}

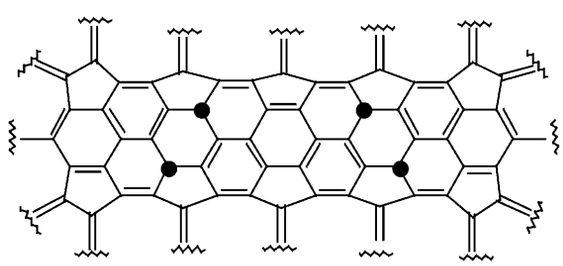

$C_{70}Ph_4$ isomer c, Energy 992.348 kcal mol^{-1}

Fig. 3 The waist section of the three isomers of $C_{70}Ph_4$ showing phenyl sites (●) that satisfy the NMR data. The phenyl rings are labelled A and B in the preferred isomer (structure a). The energy values (kcal mol^{-1}) were calculated by optimising the structures using a silicon Graphics Indy 2000 workstation.

have two sets of 1,4-situated phenyl groups, which span six-membered rings of the [70]fullerene cage. From the data available, however, it is not possible to establish the relationship about the symmetry plane of one set of two phenyl groups with the other. The only additional requirement to assist with predicting the molecular structure is, therefore, that each set of 1,4-situated phenyl groups must be located so as to generate a C_s symmetrical product. There are three possible regioisomers that satisfy the experimental data (Fig. 3). 7,19,23,37-Tetraphenyl-7,19,23,37-tetrahydro[70]fullerene (Fig. 3a) is the most likely structure for $C_{70}Ph_4$, even though it is not the lowest energy structure, as it results from sequential 1,4 substitutions, whereas the other isomers require that substitution starts at two points in $C_{70}Cl_{10}$. Using the same argument as that used in assigning the structure of $C_{70}Ph_6$, a mixture of all three isomers would result if this were to be possible, whereas the presence of only one is observed. $C_{70}Ph_4$ undergoes decomposition (probably autoxidation, as other phenylated fullerenes have been shown to oxidise producing a variety of fullerene derivatives),[11] apparently generating a single product upon storage, resulting in the presence of two multiplets in the ^{1}H NMR spectrum at $\delta = 7.539$–7.557 and 7.687–7.708. The intensities of the multiplets increase over several weeks as the signals due to the isomer of $C_{70}Ph_4$ concomitantly decrease. The structure of this oxidation product is not known at present but may be responsible for the second reduction traces observed during the electrochemical studies (*vide infra*).

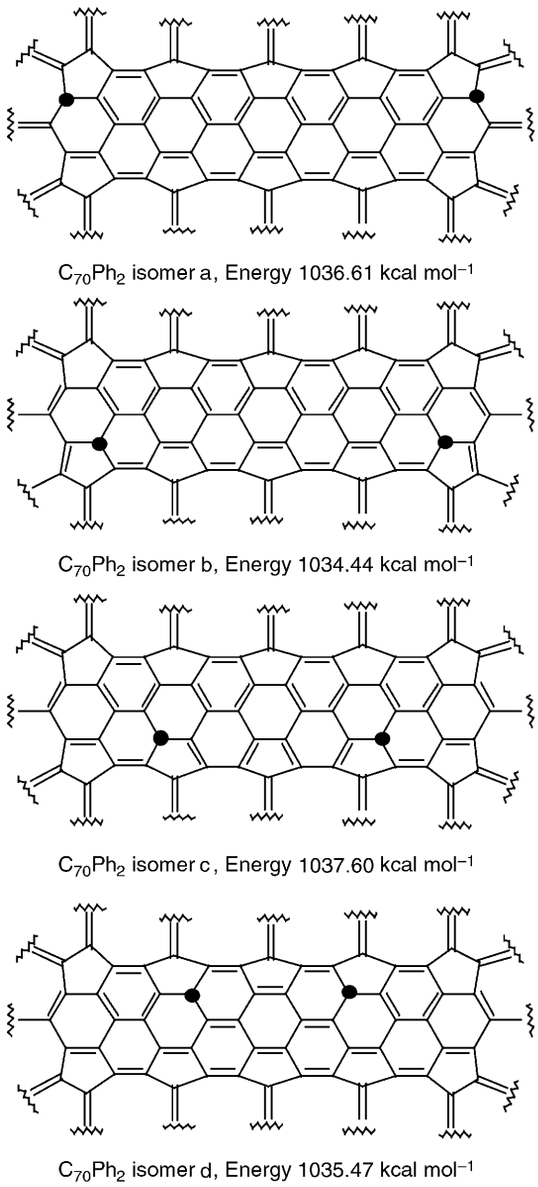

Fig. 4 The waist section of the four isomers (isomer a being the preferred product) of $C_{70}Ph_2$ showing phenyl sites (●) that satisfy the NMR data. The energy values (kcal mol^{-1}) were calculated by optimising the structures using a silicon Graphics Indy 2000 workstation.

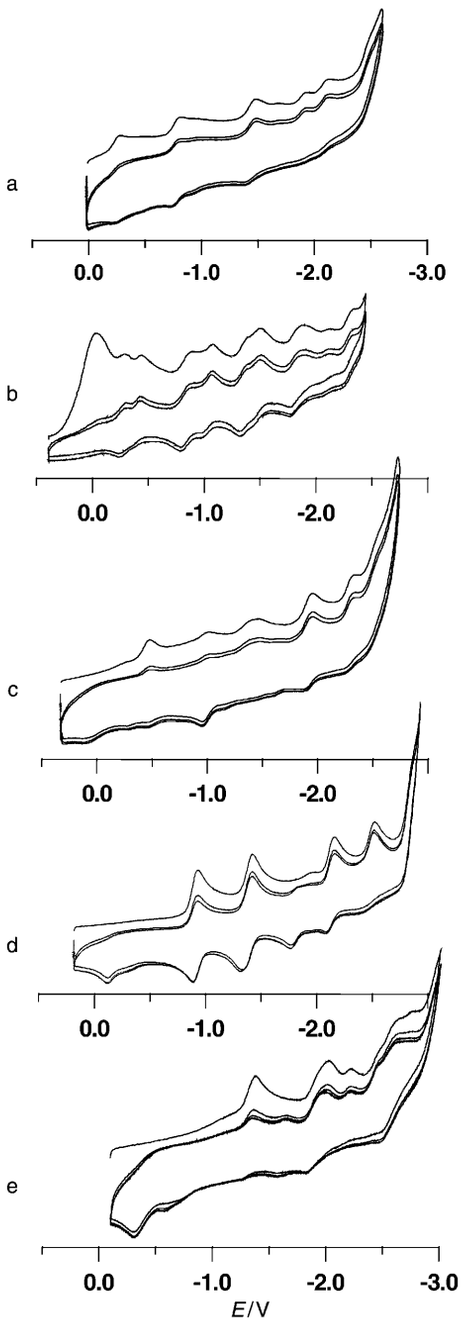

Fig. 5 Cyclic voltammetric curves for $C_{70}Ph_{2n}$, THF/TBAH solutions, scan rate = 0.5 V s^{-1}, T = 25 °C, working electrode: Pt; n = 1 (a); 2 (b); 3 (c); 4 (d) and 5 (e).

The ^{1}H NMR spectrum of $C_{70}Ph_2$ clearly shows that the molecule has C_s symmetry, because only one set (*ortho*-, *meta*- and *para*-) of proton signals are observed for the freely rotating phenyl rings. It is therefore reasonable to assume that these phenyl rings are not attached to adjacent cage carbons and are thus 1,4-situated across a hexagon. There are four possible C_s symmetric regioisomers, derived from two of the ten addition sites (Fig. 4). Using the preceding arguments it is likely that 7,19-diphenyl-7,19-dihydro[70]fullerene (Fig. 3a) is the single isomer obtained.

The cyclic voltammetric (CV) curves for $C_{70}Ph_{2n}$ (n = 1–5), in TBAH/THF solutions are collected in Fig. 5. Qualitative comparison between them shows some general trends associated with the progressive addition of phenyl groups to C_{70}. As the number of groups increases, the CV morphology diverges from that observed for C_{70} which, similarly to C_{60}, is characterized by six reversible one-electron equidistant peaks whose $E_{1/2}$ values are reported, under the same conditions as for Fig. 5, in Table 1. Modifications of the CV patterns are observed both for the number, the location of the redox processes, and the reversibility of the processes. Along the series, each reduction process occurs at potentials that become more and more negative. This trend is expected and parallels that reported for families of C_{60}, C_{70} and higher fullerenes polyadducts.[12] Importantly, however, the first reduction of $C_{70}Ph_2$ is less negative than that of the parent C_{70}.[13a] The significant 100 mV anodic shift proves that the electron-withdrawing effect exerted by the phenyl groups overcomes the destabilization of the redox orbitals caused by the removal of two π-electron-carrying atoms. A similar competition, resulting in a near balance between the opposing electronic effects, has been observed earlier for a cyano derivative of C_{60}.[13b] The same effect seems to occur in the $C_{70}Ph_4$ species but the complications observed in the CV curve makes this conclusion more ambiguous (*vide infra*). From the next species on, the destabilising effect prevails and results in an increasing cathodic shift of the reduction processes.

Table 1 $E_{1/2}$ (V *vs.* SCE) measured in THF/TBAH solutions at 25 °C; *m* is the number of added electrons

m	C_{70}	$C_{70}Ph_2$	$C_{70}Ph_4$	$C_{70}Ph_6$	$C_{70}Ph_8$	$C_{70}Ph_{10}$
1	−0.35	−0.25	−0.25[b]	−0.47	−0.91	−1.34[a]
2	−0.91	−0.79	−0.83[b]	−1.00	−1.37	−2.0
3	−1.44	−1.43	−1.35[b]	−1.6[a]	−2.13	−2.58[a]
4	−1.88	−1.93	−1.82	−2.10	−2.44[a]	
5	−2.40	−2.13	−2.30	−2.3[a]		
6	−2.86	−2.5[a]				

[a] E_p (irreversible peak). [b] Value referred to the first member of pairs.

$C_{70}Ph_2$ is also the species for which morphological changes in the CV curves are minimal with respect to C_{70}, although kinetic complications (*i.e.* ECE mechanisms), especially coupled to the fourth and following electron-transfer processes, are present. Particularly interesting is the case of $C_{70}Ph_4$. The first CV scan (Fig. 5b) shows a strong triangularly-shaped reduction located at *ca*. 0.0 V which, however, has almost disappeared in the successive scan, if performed without renewing the diffusion layer. The morphology of the peak, and the fact that its intensity is linear with the scan rate, indicates that it is derived from strongly adsorbed neutral species. The readability of the CV curve improves greatly in the following scans, where a low shoulder replaces the intense adsorption peak. The curve shows the presence of double peaks, with almost equal intensities, which might suggest the existence of (at least) two isomers having different electronic/electrochemical properties, although the presence of an autoxidation product in the starting material cannot be entirely discounted (*vide supra*). The resolution of isomers by voltammetric techniques has been previously reported in the cases of pristine C_{78} and C_{84},[14] but such an hypothesis cannot be easily verified in the present case, since the isolation of the two possible isomers has not been so far achieved. For the higher species, from $C_{70}Ph_6$ to $C_{70}Ph_{10}$, along with the increasingly negative potentials of the redox processes, one can observe (i) a decreasing number of processes and (ii) a greater instability of the reduced species. Such an instability is already evident, in the curves in Fig. 5, following the second–third reduction of these species and it results in the absence of the anodic counterpart of the reduction peaks and in the appearance of novel redox couples during successive scans, an effect ascribed to electroactive products of the reduced, and chemically modified, pristine compound, according to an ECE mechanism. Except for $C_{70}Ph_{10}$, more reversible CV patterns were in fact obtained by increasing scan rate and, in general, by limiting the inversion potential to less cathodic values. Under these conditions, the $E_{1/2}$ values reported in Table 1 were obtained.

The case of $C_{70}Ph_8$ deserves more attention: the first-scan CV curve (Fig. 5d) consists of two couples of redox processes separated by a large gap. The first three processes are reversible, while the last one is chemically irreversible, as proved by the absence of the anodic peak. Within the gap, a small cathodic shoulder is observed. Its height indicates a very low concentration of the species responsible for it in the diffusion layer. In the reverse scan, however, a more intense anodic counterpart of the low shoulder appears. This occurs after the fourth irreversible reduction and suggests that a chemical reaction produces a large amount of the relevant species after the fourth reduction. In the second and following scans, the cathodic shoulder has not increased significantly. It is therefore concluded that a dynamical process (*i.e.* a fast reversible process) links the reduced pristine species to the product responsible for the additional peak. Further work, aimed at better elucidating this process and identifying the species, is underway.

Finally, the $E_{1/2}$ and peak potential (E_p, for the irreversible processes) for the redox processes observed, for all the species considered, are collected in Table 1 and shown in Fig. 6.

Table 2 LUMO energies (hartree) of C_{70} and $C_{70}Ph_{2n}$ (n = 1–5)

	MM3/MNDO	MM3/PM3	MNDO	PM3
C_{70}	−0.1073	−0.1200	−0.1044	−0.1173
$C_{70}Ph_2$	−0.1085	−0.1233	−0.1048	−0.1218
$C_{70}Ph_4$	−0.0975	−0.1094	−0.0937	−0.1064
$C_{70}Ph_6$	−0.1071	−0.1201	−0.1048	−0.1193
$C_{70}Ph_8$	−0.0771	−0.0878	−0.0738	−0.0854
$C_{70}Ph_{10}$	−0.0635	−0.0733	−0.0587	−0.0698

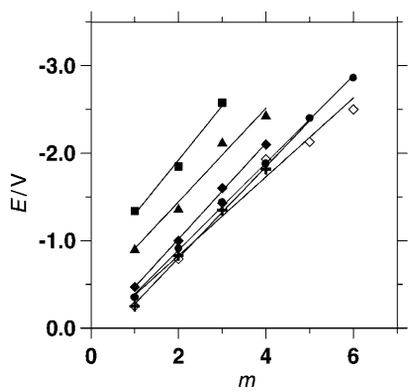

Fig. 6 Graphical display of data gathered in Table 1, relative to the reduction processes for $C_{70}Ph_{2n}$ (n = 1–5): $E_{1/2}$ (E_p) *vs.* the number of added electrons (*m*); (●) C_{70}; (◇) $C_{70}Ph_2$; (+) $C_{70}Ph_4$; (◆) $C_{70}Ph_5$; (▲) $C_{70}Ph_8$; (■) $C_{70}Ph_{10}$.

The interplay between the electron-attracting effect of the phenyl groups, that increases the reduction potential of the first two phenylated compounds, and the cage saturation caused by the insertion, that decreases the potential, can be simulated (to zeroth-order) by the calculation of the lowest unoccupied molecular orbital (LUMO) energies. Such energies are a function of the same two effects and their systematic evaluation can shed further light on how the phenyls and cage interact. Table 2 shows the LUMO energies for the six compounds (C_{70} plus all of the $C_{70}Ph_{2n}$) calculated with two semi-empirical models (MNDO and PM3) using the molecular geometries optimised with molecular mechanics and the same two semi-empirical procedures. MM3 was employed because the phenyl–phenyl interactions are mainly of the van der Waals type, for which the model was explicitly and carefully parametrised. By contrast, Hartree–Fock models generally barely include dispersion forces and the optimised geometries may be inaccurate.

Table 2 readily shows that the diphenylated system is more easily reduced than C_{70}. In general, the results are independent of the optimization model used. However, optimization with MM3 and subsequent molecular orbital calculations provide energies consistently slightly lower than the full semiempirical treatment with either MNDO or PM3. Variation of the energies is not entirely surprising because phenyl rotation can strongly affect the through-space and through-bond interactions of the π-electron of the phenyl shell with those of the cage.

Another interesting property of these species can be grasped by inspection of Fig. 7, which shows the charge distribution calculated for the tetra-anion of $C_{70}Ph_{10}$. The system was selected because of the presence of two shells (cage and phenyls) and because the effect, already present at lower charging and for a lower number of phenyls, is more pronounced here. In short, calculations show that concentric spheres of charge are formed in the tetra-anion, from which it may be concluded that addition of carefully chosen addends at selective points of the fullerene cage and subsequent charging of these species may afford otherwise unobtainable charge distributions at the molecular level.

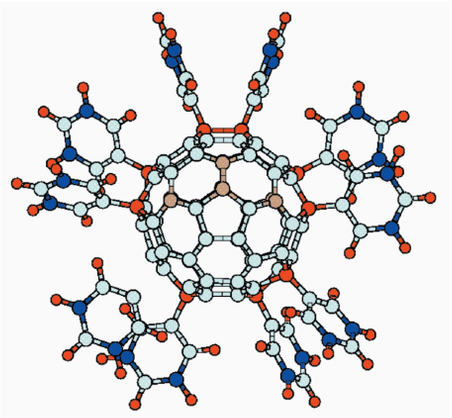

Fig. 7 Charge distribution in the tetra-anion of $C_{70}Ph_{10}$, negative charge in blue, positive charge in red.

Conclusions

$C_{70}Ph_{2n}$ (n = 1–5) compounds cover a wide range of properties. Although the π-electron pattern of the cage of the lowest members of this poly-phenylated fullerene series is rather similar to that of pristine C_{70}, they have a lower reduction potential, which makes the diphenylated and tetraphenylated species ideal candidates as some of the best electron-accepting systems based on stable molecules. In the highest members of the series, charge injections create concentric shells of charges. Since the phenyl–cage interactions can be affected by changing the number of phenyls, their location and, in the future, their substituents, it is anticipated that these effects will be exploited to create a wide range of molecular responses that could be of interest in practical applications.

Acknowledgements

We acknowledge financial support of this work by EPSRC and the TMR initiative of the European Union under contract FMRX-CT97-0126 on Usable Fullerene Derivatives (USEFULL). J. O. L. was the recipient of an eight-months TMR-USEFULL scholarship in Bologna. P. R. B. acknowledges the EPSRC for the award of an Advanced Fellowship. The University of Bologna group also acknowledges partial support from CNR by programme "Materiali Innovativi (legge 95/95)".

References

1 See for instance, M. Fanti, G. Orlandi and F. Zerbetto, *J. Phys. Chem. A*, 1997, **101**, 3015.
2 (*a*) R. D. Johnson, C. S. Yannoni, H. C. Dorn, J. R. Salem and D. S. Bethune, *Science*, 1992, **255**, 1235; (*b*) R. Tycko, R. C. Haddon, G. Dabbagh, S. H. Glarum, D. C. Douglass and A. M. Mujsce, *J. Phys. Chem.*, 1991, **95**, 518; (*c*) C. S. Yannoni, R. D. Johnson, G. Mejer, D. S. Bethune and J. R. Salem, *J. Phys. Chem.*, 1991, **95**, 9; (*d*) J. E. Fischer, P. A. Heiney and A. B. Smith III, *Acc. Chem. Res.*, 1992, **25**, 112; (*e*) H. He, J. Barras, J. Foulkes and J. Klinowski, *J. Phys. Chem. B*, 1997, **101**, 117; (*f*) X. Shang, M. H. Issa and A. A. Rodriguez, *J. Phys. Chem. A*, 1998, **102**, 7731.
3 (*a*) P. R. Birkett, A. G. Avent, A. D. Darwish, H. W. Kroto, R. Taylor and D. R. M. Walton, *J. Chem. Soc., Chem. Commun.*, 1995, 683; (*b*) P. R. Birkett, A. G. Avent, A. D. Darwish, H. W. Kroto, R. Taylor and D. R. M. Walton, *Tetrahedron*, 1996, **52**, 5235.
4 M. Carano, P. Ceroni, L. Mottier, F. Paolucci and S. Roffia, *J. Electrochem. Soc.*, 1999, **146**, 3357.
5 (*a*) N. L. Allinger, Y. H. Yuh and J.-H. Lii, *J. Am. Chem. Soc.*, 1989, **23**, 8551; (*b*) J.-H. Lii and N. L. Allinger, *J. Am. Chem. Soc.*, 1989, **23**, 8566; (*c*) J.-H. Lii and N. L. Allinger, *J. Am. Chem. Soc.*, 1989, **23**, 8576.
6 (*a*) J. Ponder and F. Richards, *J. Comput. Chem.*, 1987, **8**, 1016; (*b*) C. Kundrot, J. Ponder and F. Richards, *J. Comput. Chem.*, 1991, **12**, 402; (*c*) M. J. Dudek and J. Ponder, *J. Comput. Chem.*, 1995, **16**, 791.
7 (*a*) D. A. Leigh, A. Murphy, J. P. Smart, M. S. Deleuze and F. Zerbetto, *J. Am. Chem. Soc.*, 1998, **120**, 6458; (*b*) B. Paci, M. S. Deleuze, R. Caciuffo, J. Tomkinson, F. Ugozzoli and F. Zerbetto, *J. Phys. Chem. A*, 1998, **102**, 6910; (*c*) R. Caciuffo, A. Degli Esposti, M. S. Deleuze, D. A. Leigh, A. Murphy, B. Paci, S. Parker and F. Zerbetto, *J. Chem. Phys.*, 1998, **109**, 11094; (*d*) M. S. Deleuze, D. A. Leigh and F. Zerbetto, *J. Am. Chem. Soc.*, 1999, **121**, 2364; (*e*) M. S. Deleuze and F. Zerbetto, *J. Am. Chem. Soc.*, 1999, **121**, 5281.
8 M. J. S. Dewar and W. Thiel, *J. Am. Chem. Soc.*, 1977, **99**, 4907.
9 M. J. Frisch, G. W. Trucks, H. B. Schlegel, P. M. W. Gill, B. G. Johnson, M. A. Robb, J. R. Cheeseman, T. Keith, G. A. Petersson, J. A. Montgomery, K. Raghavachari, M. A. Al-Laham, V. G. Zakrzewski, J. V. Ortiz, J. B. Foresman, C. Y. Peng, P. Y. Ayala, W. Chen, M. W. Wong, J. L. Andres, E. S. Replogle, R. Gomperts, R. L. Martin, D. J. Fox, J. S. Binkley, D. J. Defrees, J. Baker, J. P. Stewart, M. Head-Gordon, C. Gonzalez and J. A. Pople, Gaussian, Inc., Pittsburgh, PA, 1995.
10 The derivatives are numbered using the IUPAC system; E. W. Godly and R. Taylor, *Pure Appl. Chem.*, 1997, **69**, 1411.
11 (*a*) P. R. Birkett, A. G. Avent, A. D. Darwish, H. W. Kroto, R. Taylor and D. R. M. Walton, *J. Chem. Soc., Chem. Commun.*, 1995, 1869; (*b*) A. G. Avent, P. R. Birkett, A. D. Darwish, H. W. Kroto, R. Taylor and D. R. M. Walton, *Chem. Commun.*, 1997, 1579.
12 (*a*) C. Boudon, J.-P. Gisselbrecht, M. Gross, L. Isaacs, H. L. Anderson, R. Faust and F. Diederich, *Helv. Chim. Acta*, 1995, **78**, 1334; (*b*) F. Cardullo, P. Seiler, L. Isaacs, J.-F. Nierengarten, R. F. Haldimann, F. Diederich, T. Mordasini-Denti, W. Thiel, C. Boudon, J.-P. Gisselbrecht and M. Gross, *Helv. Chim. Acta*, 1997, **80**, 343; (*c*) C. Boudon, J.-P. Gisselbrecht, M. Gross, A. Herrmann, M. Rüttiman, J. Crassous, F. Cardullo, L. Echegoyen and F. Diederich, *J. Am. Chem. Soc.*, 1998, **120**, 7860; (*d*) *Fullerenes and related Structures*, ed. A. Hirsch, Springer-Verlag, Berlin, 1999.
13 (*a*) For examples of enhanced electron accepting properties in C_{60} derivatives see: T. Da Ros, M. Prato, M. Carano, P. Ceroni, F. Paolucci and S. Roffia, *J. Am. Chem. Soc.*, 1998, **120**, 11645; D. M. Guldi, H. Hüngerbuhler and K.-D. Asmus, *J. Phys. Chem. A*, 1997, **101**, 1783; (*b*) M. Kerchavarz, B. Knight, G. Srdanov and F. Wudl, *J. Am. Chem. Soc.*, 1995, **117**, 11371.
14 L. Echegoyen and L. E. Echegoyen, *Acc. Chem. Res.*, 1998, **31**, 593.